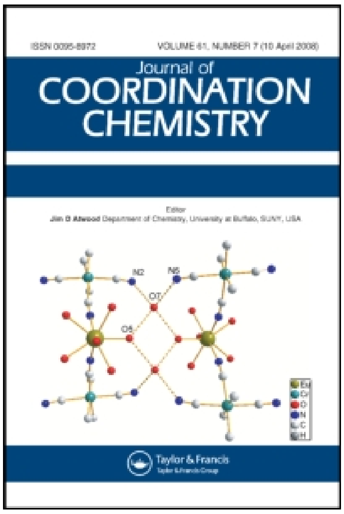

**Journal of Coordination Chemistry**
Publication details, including instructions for authors and subscription information:
http://www.informaworld.com/smpp/title~content=t713455674

# Synthesis, spectroscopic investigations, and biological activity of metal complexes of *N*-benzoylthiosemicarbazide

Adel A. A. Emara[a]; H. S. Seleem[a]; Aml M. Madyan[a]
[a] Faculty of Education, Department of Chemistry, Ain Shams University, Roxy, Cairo 11341, Egypt

**To cite this Article** Emara, Adel A. A. , Seleem, H. S. and Madyan, Aml M.(2009) 'Synthesis, spectroscopic investigations, and biological activity of metal complexes of *N*-benzoylthiosemicarbazide', Journal of Coordination Chemistry, 62: 15, 2569 — 2582

**To link to this Article: DOI:** 10.1080/00958970902866538

**URL:** http://dx.doi.org/10.1080/00958970902866538

*Journal of Coordination Chemistry*
Vol. 62, No. 15, 10 August 2009, 2569–2582

# Synthesis, spectroscopic investigations, and biological activity of metal complexes of *N*-benzoylthiosemicarbazide

ADEL A.A. EMARA*, H.S. SELEEM and AML M. MADYAN

Faculty of Education, Department of Chemistry, Ain Shams University, Roxy,
Cairo 11341, Egypt

(*Received 14 May 2008; in final form 11 December 2008*)

*N*-Benzoylthiosemicarbazide, HL, was obtained by fusion of benzoylhydrazide and ammonium thiocyanate. Reactions of HL with cobalt(II), nickel(II), copper(II), zinc(II), iron(III), cadmium(II), oxovanadium(IV), and dioxouranium(VI) in 1 : 1 molar ratio yield the corresponding complexes. The *N*-benzoylthiosemicarbazide may act as a neutral or monobasic bidentate ligand coordinated through NS or NO sites. The structures of the HL ligand and its complexes were identified by elemental analysis, infrared, electronic, mass, $^1$H-NMR, and ESR spectra as well as magnetic susceptibility and molar conductivity measurements. Different geometries were obtained for the metal complexes. The ligand and its metal complexes were investigated for antibacterial and antifungal properties. Two Gram-positive bacteria, *Staphylococcus aureus* and *Streptococcus pyogenes*, two Gram-negative, bacteria, *Pseudomonas fluorescens* and *Pseudomonas phaseolicola* and two fungi, *Fusarium oxysporum* and *Aspergillus fumigatus*, were used in this study. The metal complexes were more effective than the free ligand.

*Keywords*: *N*-Benzoylthiosemicarbazide; Bidentate ligand; Metal complexes; Thermal analysis; ESR spectra; Antimicrobial activity

## 1. Introduction

Semi-/thiosemi-/isosemicarbazides and their carbazones with different substituents, as well as their metal complexes, have been studied because of complexing properties [1, 2], biological activity [3–8], and analytical applications [9, 10].

Some work has been done on the transition metal complexes of substituted thiosemicarbazides [11–14]. Although, the crystal structure of the *N*-benzoylthiosemicarbazide was described [15], no publication has appeared on its metal complexes and their properties.

In this article, *N*-benzoylthiosemicarbazide was reacted with cobalt(II), nickel(II), copper(II), zinc(II), iron(III), chromium(III), cadmium(II), oxovanadium(IV), and dioxouranium(VI) ions in 1 : 1 or 1 : 2 molar ratio (ligand : metal ion) to afford metal complexes. Reaction of HL with chromium(III) ion gave oily products not possible to isolate. The metal complexes were identified by physicochemical

---

*Corresponding author. Email: adelaemara@yahoo.com

*Journal of Coordination Chemistry*
ISSN 0095-8972 print/ISSN 1029-0389 online © 2009 Taylor & Francis
DOI: 10.1080/00958970902866538

and spectroscopic techniques. The *N*-benzoylthiosemicarbazide is a neutral bidentate or monobasic bidentate ligand, coordinated through NS or NO sites. Cobalt(II), nickel(II), iron(III), and oxovanadium(IV) complexes are octahedral; nitrate is unidentate in iron(III) complex and sulfate is bidentate in the oxovanadium(IV) complex. Zinc(II) and cadmium(II) complexes are tetrahedral, while copper(II) is square planar with two unidentate nitrates in the coordination sphere. The dioxouranium(VI) complex has a coordination number eight.

The antimicrobial and antifungal activities of the ligand and of the complexes towards *Staphylococcus aureus* and *Streptococcus pyogenes* as Gram-positive, *Pseudomonas fluorescens* and *Pseudomonas phaseolicola* as Gram-negative and *Fusarium oxysporum* and *Aspergillus fumigatus* fungi were determined.

## 2. Experimental

### 2.1. *Materials*

Ethyl benzoate, hydrazine monohydrate, Co(II), Ni(II), Cu(II), Zn(II), Fe(III), and Cd(II) ions were used as nitrate salts and were Merck or BDH. Oxovanadium(IV) sulfate monohydrate and dioxouranium(VI) acetate dihydrate were from Fluka. Organic solvents (absolute ethanol, ethanol, methanol, isopropyl alcohol) and triethylamine were reagent grade.

### 2.2. *Synthesis of* N-*benzoylthiosemicarbazide ligand*

*N*-benzoylthiosemicarbazide, HL, ligand was synthesized in two steps. The first was preparation of benzoylhydrazide by condensation of ethyl benzoate ester (1.502 g, 10.00 mmol) in 20 mL absolute ethanol with hydrazine monohydrate (0.500 g, 10.00 mmol) in 20 mL absolute ethanol in the molar ratio 1 : 1. The reaction was heated to reflux for 12 h. A white precipitate formed on cooling the solution to room temperature and was collected by filtration. White crystals were obtained by recrystallization with isopropyl alcohol. The yield was 1.701 g (85.47%) and the melting point was 115°C. The second step was fusion of the formed benzoylhydrazide (1.360 g, 10.00 mmol) with ammonium thiocyanate (0.761 g, 10.00 mmol), cooling to room temperature and adding drops of water and concentrated hydrochloric acid. White precipitate formed and was collected by filtration. White crystals were obtained by recrystallization with DMF/water. The yield was 1.202 g (75.3%) and the melting point was 182°C. Scheme 1 illustrates the synthesis of *N*-benzoylthiosemicarbazide, HL, ligand.

### 2.3. *Synthesis of* N-*benzoylthiosemicarbazide metal complexes*

A methanolic solution of HL was added gradually to methanolic solutions of metal salts in the molar ratio 1 : 1 and/or 1 : 2 (metal ion : ligand) with constant stirring for 0.5 to 1 h and the reaction was refluxed for 2–10 h, where the solid complexes precipitated and were filtered off, washed with methanol, ether and air dried. This reaction was

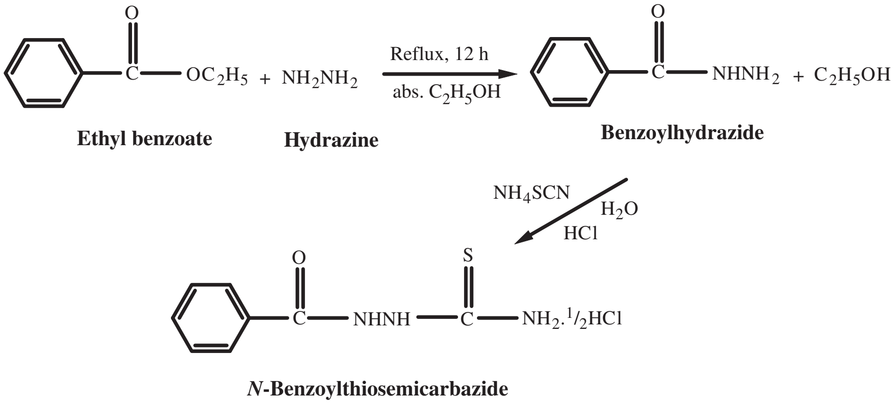

Scheme 1. Synthesis of the *N*-benzoylthiosemicarbazide.

successful for copper(II), iron(III), and oxovanadium(IV). An alternative synthetic approach is the addition of triethylamine as a deprotonating agent to the ligand in the molar ratio 1 : 1. Then the deprotonated ligand reacts with metal salts to yield the corresponding complexes. The complexes of nickel(II), cobalt(II), zinc(II), cadmium(II), and dioxouranium(VI) ions were obtained by this method. The following detailed two preparations are given as examples, and the other complexes were obtained similarly. The conditions of the reactions of the metal salts with the HL ligand are listed in table 1.

**2.3.1. Synthesis of nickel(II) complex, (2).** A solution of triethylamine (1.011 g, 10.00 mmol) in 15 mL methanol was added gradually to a solution of *N*-benzoylthiosemicarbazide ligand (1.950 g, 10.00 mmol) in 30 mL methanol then heated to reflux for 30 min to affect deprotonation. A solution of $Ni(NO_3)_2 \cdot 6H_2O$ (1.450 g, 5.00 mmol) in 25 mL methanol was added gradually to the deprotonated ligand with constant stirring for 1 h at room temperature then refluxed for 5 h. Dark green precipitate formed while hot and was filtered off, washed with methanol, then air dried. The yield was 1.531 g (58.2%) and its melting point was higher than 260°C.

**2.3.2. Synthesis of copper(II) complex, (3).** Copper(II) nitrate tetrahydrate, $Cu(NO_3)_2 \cdot 3H_2O$ (1.208 g, 5.00 mmol) in 25 mL methanol was added gradually with constant stirring to solution of HL (0.975 g, 5.00 mmol) in 30 mL methanol. The solution was stirred for 1 h and then heated to reflux for 4 h. Dark blue precipitate formed after cooling to room temperature, was filtered off, washed with methanol and air dried. The yield was 1.316 g (59%) and its melting point was higher than 260°C.

## 2.4. *Physical measurements*

Carbon, hydrogen, nitrogen, and sulfur analyses were carried out at the Microanalytical Center, Cairo University, Giza, Egypt. Metal ions were analyzed after dissolution of the solid complex in hot concentrated nitric acid, $HNO_3$, diluting with distilled water and

Table 1. Physical and analytical data for *N*-benzoylthiosemicarbazide ligand and its metal complexes.

| | | | | | | | | Elemental analyses; Calcd (found) | | | | |
|---|---|---|---|---|---|---|---|---|---|---|---|---|
| | Reactions of the ligand and metal salts | Wt. of the ligand, g (mmol) | Wt. of the metal salt, g (mmol) | Molecular formula (molecular weight) | Yield *g* (%) | m.p. (°C) | Color | C (%) | H (%) | N (%) | S (%) | M (%) |
| | $HL \cdot ½HCl$[a] | – | – | $C_8H_{9.5}N_3OSCl_{0.5}$<br>213.475 | 1.202<br>(75.3) | 182 | White | 45.01<br>(44.80) | 4.49<br>(4.58) | 19.68<br>(19.63) | 15.02<br>(15.07) | –<br>– |
| **(1)** | $HL + Co(NO_3)_2 \cdot 6H_2O \rightarrow$<br>$[Co(L)_2(H_2O)_2] \cdot 2H_2O$[b] | 1.950<br>(10.0) | 1.096<br>(5.00) | $C_{16}H_{24}N_6O_6S_2Co$<br>519.467 | 1.454<br>(43.4) | >260 | Olive green | 37.00<br>(36.81) | 4.66<br>(4.55) | 16.18<br>(16.27) | 12.35<br>(12.38) | 11.35<br>(11.66) |
| **(2)** | $HL + Ni(NO_3)_2 \cdot 6H_2O \rightarrow$<br>$[Ni(L)_2(H_2O)_2] \cdot 2CH_3OH$[b] | 1.950<br>(10.0) | 1.450<br>(5.00) | $C_{18}\ H_{28}N_6O_6S_2Ni$<br>547.278 | 1.531<br>(58.2) | >260 | Dark green | 39.51<br>(39.74) | 5.16<br>(4.93) | 15.36<br>(15.53) | 11.72<br>(11.56) | 10.72<br>(10.93) |
| **(3)** | $HL + Cu(NO_3)_2 \cdot 3H_2O \rightarrow$<br>$[Cu(HL)(NO_3)_2] \cdot CH_3OH$[b] | 0.975<br>(5.00) | 1.208<br>(5.00) | $C_8H_{13}N_5O_8SCu$<br>410.230 | 1.316<br>(59.1) | >260 | Dark blue | 26.35<br>(26.47) | 3.19<br>(3.28) | 17.07<br>(16.90) | 7.82<br>(7.69) | 14.37<br>(14.32) |
| **(4)** | $HL + Zn(NO_3)_2 \cdot 6H_2O \rightarrow$<br>$[Zn(L)_2] \cdot 2H_2O$[c] | 1.950<br>(10.0) | 1.487<br>(5.00) | $C_{16}H_{20}N_6O_4S_2Zn$<br>484.880 | 1.535<br>(63.3) | >260 | White | 39.23<br>(39.22) | 4.12<br>(4.16) | 17.16<br>(17.08) | 13.09<br>(13.15) | 13.35<br>(13.25) |
| **(5)** | $HL + Fe(NO_3)_3 \cdot 9H_2O \rightarrow$<br>$[Fe(L)(NO_3)_2(H_2O)_2] \cdot 2C_2H_5OH$[b] | 0.975<br>(5.00) | 1.454<br>(5.00) | $C_{12}H_{24}N_5O_{11}SFe$<br>502.263 | 1.090<br>(43.4) | >260 | Brown orange | 28.70<br>(28.72) | 4.82<br>(4.97) | 13.94<br>(13.71) | 6.38<br>(6.79) | 11.12<br>(11.28) |
| **(6)** | $HL + Cd(NO_3)_2 \cdot 6H_2O \rightarrow$<br>$[Cd(L)_2] \cdot 1^1/_2H_2O$[c] | 1.950<br>(10.0) | 1.722<br>(5.00) | $C_{16}H_{19.5}N_6O_{3.5}S_2Cd$<br>528.400 | 1.284<br>(48.6) | >210 | White | 36.37<br>(36.33) | 3.72<br>(3.60) | 15.91<br>(15.91) | 12.14<br>(12.03) | 21.27<br>(21.23) |
| **(7)** | $HL + VOSO_4 \cdot H_2O \rightarrow$<br>$[VO(HL)(SO_4)(H_2O)] \cdot 2CH_3OH$[b,d] | 0.975<br>(5.00) | 0.905<br>(5.00) | $C_{10}H_{18}N_3O_9S_2V$<br>439.339 | 0.997<br>(45.4) | >260 | Dark blue | 27.34<br>(27.24) | 4.13<br>(4.30) | 9.56<br>(9.69) | 14.60<br>(14.20) | – |
| **(8)** | $HL + UO_2(CH_3COO)_2 \cdot 2H_2O \rightarrow$<br>$[UO_2(L)_2(H_2O)_2] \cdot 2H_2O$[c] | 1.950<br>(10.0) | 2.000<br>(5.00) | $C_{16}H_{24}N_6O_8S_2U$<br>730.563 | 1.399<br>(38.3) | >260 | Brown | 26.31<br>(26.41) | 3.31<br>(3.22) | 11.50<br>(11.67) | 8.78<br>(8.69) | – |

[a] Elemental analysis for the chloride: Calcd/Found%; 8.30 (8.45)%.
[b] The reactions were heated to reflux for 2–4 h.
[c] The reaction was heated to reflux for 10 h.
[d] The oxovanadium(IV) sulfate was dissolved in minimum water and 30 mL methanol was added.

filtering to remove the precipitated ligand. The solution was neutralized with ammonia and the metal ions were titrated with EDTA [16–18]. FT-IR spectra (4000–400 $cm^{-1}$) of the compounds were recorded as KBr discs using FT-IR (Shimadzu) spectrophotometer model 4000. The electronic spectra (200–900) were obtained on a JASCO model V-550, UV-Vis spectrophotometer. The $^1$H-NMR spectra were obtained on a Varian Gemini 200 MHz spectrophotometer. ESR spectra were recorded on a Bruker Model EMX, X-band spectrometer. The magnetic field was calibrated with a 2,2′-diphenyl-1-picrylhydrazyl (DPPH) sample. Mass spectra were carried out by a Shimadzu-GC-MS-QL mass spectrometer model 1000 EX using a direct inlet system. TGA curves were obtained using NETZSCH-gerateban Bestell-Nr34872c Thermal Analyzer equipped with a thermobalance. The sample ($\sim$50 mg) was heated at 5°C $min^{-1}$ in a dynamic $N_2$ atmosphere. The sample was contained in a boat-shaped platinum pan suspended in the center of a furnace. Magnetic susceptibilities were measured at room temperature using a magnetic susceptibility balance (Johnson Matthey Alfa product, Model No. MKI). Diamagnetic correction was calculated from Pascal's constants [19]. Molar conductances of $10^{-3}$ M solutions of the complexes in DMF were measured on a Corning conductivity meter NY 14831 model 441 (USA).

### 2.5. *Biological activity*

The standardized disc–agar diffusion method [20] was followed to determine activity of the synthesized compounds against *S. aureus* (ATCC 25923) and *S. pyogenes* (ATCC 19615), *P. fluorescens* (S 97), *P. phaseolicola* (GSPB 2828), *F. oxysporum*, and *A. fumigatus*. Chloramphencol, cephalothin, and cycloheximide were used as standard references for Gram-positive, Gram-negative bacteria, and antifungal.

Tested compounds were dissolved in DMF (which has no inhibition activity) at 2 mg $mL^{-1}$ and 1 mg $mL^{-1}$. The test was performed on potato dextrose agars (PDA), which contain 200 g potatoes, 6 g dextrose, and 15 g agar [21]. Uniform size filter paper disks (3 disks per compound) were impregnated by equal volume (10 µL) from the specific concentration of dissolved tested compounds and carefully placed on incubated agar surface.

After incubation for 36 h at 27°C for bacteria and for 48 h at 24°C for fungi, inhibition evidenced by clear zone surround each disk was measured and used to calculate mean inhibition zone [20, 21]. Activities are categorized as: (i) low activity = mean of zone diameter $\leq 1/3$ of mean zone diameter of control, (ii) intermediate activity = mean of zone diameter $\leq 2/3$ of mean zone diameter of control, and (iii) high activity = mean of zone diameter $> 2/3$ of mean zone diameter of control.

## 3. Results and discussion

### 3.1. N-*benzoylthiosemicarbazide, HL, ligand*

The *N*-benzoylthiosemicarbazide was characterized by elemental analysis, and infrared, electronic, mass, and $^1$H-NMR spectra, existing as $HL \cdot ½HCl$. The physical and analytical data for the ligand and metal complexes are listed in table 1. The *N*-benzoylthiosemicarbazide may be either a neutral bidentate ligand with NO

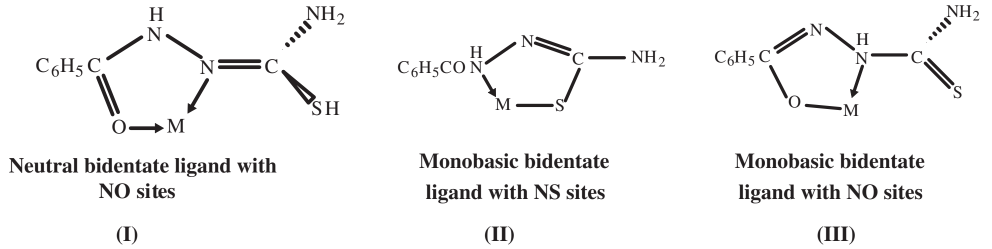

Figure 1. Coordination sites of HL with metal ions.

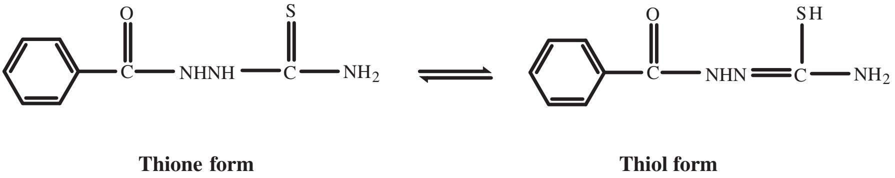

Figure 2. Tautomeric forms of the HL · 1/2 HCl ligand.

donors or monobasic bidentate with NS or NO donors. Figure 1 illustrates the representation of the proposed coordination sites of HL with metal ions. Form II is favorable for most complexes, while form I is favorable only in coordination with copper(II) and oxovanadium(IV); form III is less favorable and was not taken in consideration in complex formations.

The assignments of the vibrational frequencies were aided by comparison with the infrared frequencies of the precursors (benzoylhydrazide and ammonium thiocyanate) and other related compounds [22, 23]. There are three main features in the infrared spectra of the HL · ½HCl ligand, $\nu(NH_2)$ stretching frequency of the benzoylhydrazide at 3230–3218 $cm^{-1}$ disappeared in the infrared spectrum of the HL ligand, and new absorptions at 3417 and 3275 $cm^{-1}$ in the free ligand are assigned to the new $\nu(NH_2)$. This indicates that reaction between benzoylhydrazide and ammonium thiocyanate occurred. Also, appearance of a strong absorption at 1261 $cm^{-1}$, attributed to $\nu(C=S)$ confirms formation of C=S and appearance of a new absorption at 2053 $cm^{-1}$ was assigned to $\delta(N–C=S)$.

The mass spectrum of the HL · ½HCl ligand revealed the molecular ion peak at $m/e$ 196, coincident with the formula weight (M.Wt. = 195.211) after removal of ½ HCl.

In the $^1H$-NMR spectra of HL in DMSO-$d_6$ it exists in thione and thiol forms. Figure 2 represents the tautomeric forms of HL · ½HCl. The chemical shifts of the proton signals of HL and $[Zn(L)_2] \cdot 2H_2O$ (**4**) with their assignments are listed in "Supplementary material". The $^1H$-NMR spectra of the ligand showed signals at 9.3 and 10.5 ppm assigned to the protons of amino NH groups and 2.5 ppm assigned to the thiol. Signals at 7.4, 7.5, and 7.9 ppm were assigned to the aromatic ring. Signals at 9.3 ppm and 10.5 ppm completely disappeared on addition of $D_2O$ while the other signals persist at the same positions. It is not possible to differentiate between the thione and thiol forms from $^1H$-NMR spectra except in the aromatic range 7.0–8.6 ppm;

strong multiplets at 7.8 ppm may be due to aromatic protons of the thione. Also, two weak multiplets at 7.1 and 7.3 ppm may be due to aromatic protons of the thiol. The integrated ratio between the aromatic protons' signals of the thione and thiol forms are 92 : 8.

The electronic spectrum of the *N*-benzoylthiosemicarbazide, HL, in DMF (table 2) exhibits four absorptions at 245, 226, 215, and 203 nm. The former two correspond to ($^1L_a \rightarrow {}^1A_1$) and ($^1L_b \rightarrow {}^1A_1$) transitions of the phenyl group [24], the third band corresponds to the ($\pi \rightarrow \pi^*$) transition of C=O, and the last band corresponds to ($n \rightarrow \pi^*$) transition of the oxygen, nitrogen, and sulfur [25, 26].

From the infrared, electronic, mass, $^1$H-NMR spectra, and elemental analysis, the expected structure of *N*-benzoylthiosemicarbazide and HL · ½ HCl ligand are shown in figure 1 with molecular formula $C_8H_{9.5}N_3OSCl_{0.5}$.

### 3.2. *Complexes of the* N-*benzoylthiosemicarbazide, HL, ligand*

HL reacts with cobalt(II), nickel(II), copper(II), zinc(II), iron(III), cadmium(II), oxovanadium(IV), and dioxouranium(VI) ions to yield the corresponding metal complexes. The complexes were investigated by elemental analysis, electronic, $^1$H-NMR, mass and ESR spectra, thermal gravimetric analysis (TGA), and magnetic and molar conductivity measurements. Attempts to isolate single crystals for the metal complexes were unsuccessful.

**3.2.1. Infrared spectra of *N*-benzoylthiosemicarbazide complexes.** The characteristic vibrational frequencies and their tentative assignments are listed in table 3. The assignments were aided by comparison with the vibrational frequencies of the free ligand [11, 12].

There are four characteristic features in infrared spectra of the complexes. The first is the thioamide group –NH(C=S)NH$_2$ with a strong band at 2053 cm$^{-1}$ due to $\nu$(N–C=S) in infrared spectra of the free ligand, which disappeared in the metal complexes indicating chelation occurred by the thiol form (figure 1; form II). The second feature is the presence of coordinated water and/or methanol with a broad absorption at 3491–3400 cm$^{-1}$ due to stretching of OH; also, a band near 1600 cm$^{-1}$ is due to deformation of water. Bands at 930 and 785 cm$^{-1}$ may be attributed to rocking and wagging modes of coordinated water molecule. Existence of coordinated and uncoordinated water molecule in the complexes is confirmed by elemental analysis as well as TGA. The third feature is weak bands in the range 600–410 cm$^{-1}$, assigned to $\nu$(M–O) and $\nu$(M–N). The $\nu$(M–S) bands are expected at 300 cm$^{-1}$, out of the range of the instrument. The fourth feature is coordination nitrate and sulfate. The $NO_3^-$ ions are coordinated to Cu(II) (**3**) and Fe(III) (**5**) as a unidentate ligand with $C_{2v}$ symmetry showing three vibrational bands ($\nu_s$, $\nu'_s$, and $\nu_{as}$) which appeared at 1431–1434, 1351–1354, and 831–837 cm$^{-1}$ [27]. The $SO_4^{-2}$ is coordinated as a bidentate ligand in [VO(HL)(SO$_4$)(H$_2$O)] · 2CH$_3$OH (**7**) [28, 29] with $\nu_1$ and $\nu_2$ medium intensity at 1075 and 449 cm$^{-1}$, respectively, and $\nu_3$ and $\nu_4$ at 1270 and 625 cm$^{-1}$. The IR spectrum of **7** displayed a band at 930 cm$^{-1}$ with no counterpart in the spectrum of the ligand, assigned to (V=O). Also, the IR spectrum of dioxouranium(VI) complex (**8**) displayed a strong band at 901 cm$^{-1}$, assigned to $\nu$(O=U=O) [29].

Table 2. Electronic transition bands, magnetic moments, and molar conductance of *N*-benzoylthiosemicarbazaide and its metal complexes.

| | Electronic absorption bands (nm) and their assignments[a] | | | | | | | |
|---|---|---|---|---|---|---|---|---|
| Ligand/complexes | $^1L_a \rightarrow {}^1A_1$ (phenyl ring) | $^1L_a \rightarrow {}^1A_1$ (phenyl ring) | $\pi$–$\pi$* (C=N) | $n \rightarrow \pi$* and CT | d–d transition | d–d transition assignments | $\mu_{eff}$ ($\mu$B) | $\Lambda$[b] |
| HL · $^1/_2$HCl | 230 (0.87) | 324 (0.85) | 374 (0.46) | 410 (0.52) | – | – | – | – |
| **1** | 222 (0.91) | 310 (0.86) | 370 (0.56) | 404 (0.39) | 615 (0.02) sh,<br>490 (0.06) | $^4A_2g\ (F) \leftarrow {}^4T_1g\ (F)$<br>$^4T_1g\ (P) \leftarrow {}^4T_1g\ (F)$ | 5.09 | 9 |
| **2** | 218 (0.72) | 321 (0.89) | 388 (0.33) | 411 (0.42) | 732 (0.07),<br>690 (0.05) sh | $^3T_1g(F) \leftarrow {}^3A_2g(F)$ | 2.92 | 21 |
| **3** | 217 (0.91) | 317 (0.76) | 355 (0.42) | 425 (0.33) | 565 (0.21) | $^2A_{1g} \leftarrow {}^2B_1g$, $^2B_{2g} \leftarrow {}^2B_1g$,<br>$^2E_g \leftarrow {}^2B_1g$ | 1.73 | 83 |
| **4** | 223 (0.78) | 320 (0.71) | 357 (0.34) | 420 (0.37) | – | – | – | 16 |
| **5** | 235 (0.96) | 323 (0.79) | 382 (0.48) | 423 (0.40) | 740 (0.02),<br>605 (0.03), 558 (0.02) | Charge transfer tailing from UV to visible region | 5.62 | 91 |
| **6** | 232 (0.81) | 318 (0.82) | 374 (0.53) | 400 (0.43) | – | – | – | 18 |
| **7** | 267 (0.87) | 309 (0.84) | 354 (0.43) | 418 (0.33) | 565 (0.03),<br>500 (0.02) | $^2E \leftarrow {}^2B_2$<br>$^2B_1 \leftarrow {}^2B_2$ | 2.1 | 105 |
| **8** | 225 (0.88) | 318 (0.79) | 367 (0.44) | 420 (0.27) | 512 (0.03) | | – | 18 |

[a] Values of $\varepsilon_{max}$ are in parentheses and multiplied by $10^{-4}$ (L mol$^{-1}$ cm$^{-1}$).

[b] Molar conductivities were measured in DMF at $1 \times 10^{-3}$ M. Values are in Ohm$^{-1}$cm$^2$mol$^{-1}$.

Table 3. Characteristic of vibrational frequencies ($cm^{-1}$) of HL and its metal complexes and their assignments.

| Ligand/complexes | $\nu$(OH) $H_2O$, $CH_3OH$ and/or $C_2H_5OH$ | $\nu$(NH) | $\nu$(N–C=S) | $\nu$(C=O) | $\delta(H_2O)$ | $\nu$(C–S) | $\nu$(M–N) | Other bands |
|---|---|---|---|---|---|---|---|---|
| HL · $^1/_2$HCl | – | 3300 s, 3145 s | 2053 m | 1701 s, 1684 s | – | – | – | 1261 vs, $\nu$(C=S) |
| **1** | 3490 br, m | 3297 m, 3182 m | – | 1661 w | 1606 s | 699 m | 444 w | – |
| **2** | 3426 br, m | 3332 m, 3283 m | – | – | 1605 vs | 697 m | 455 w | – |
| **3** | 3400 sh, m | 3293 s, 3188 s | – | 1667 m | 1613 s | 706 m | 432 w | 1431 s, 1351 vs, 831 m; Unidentate $NO_3^-$ |
| **4** | 3449 m | 3294 m, 3183 m | – | 1586 m | 1611 s | 698 m | 467 w | – |
| **5** | 3405 m, sh | 3297 m, 3194 m | – | – | 1605 s | 688 m | – | 1434 sh, s 1354 vs 837 m; unidentate $NO_3^-$ |
| **6** | 3491 m | 3313 m, 3279 m | – | – | 1605 vs | 711 m | 448 w | – |
| **7** | 3450 sh, m | 3282 s, 3182 s | – | 1675 s | 1618 vs | 708 m | 432 w | 930 m, $\nu$(V=O); 1270 s, 1075 m, 625 m, 449 w, bidentate $SO_4^-$ group |
| **8** | 3410 m, sh | 3240 m, 3113 s | – | 1609 m, 1591 m | 1605 s | 704 m | 444 w | 901vs, $\nu(UO_2)$ |

s, strong; m, medium; vs, very strong; sh, shoulder; br, broad.

**3.2.2. Electronic spectra, magnetic, and molar conductivity measurements.** Electronic spectra of the metal complexes were recorded in DMF from 200–900 nm. Table 2 lists the electronic spectral bands and molar conductivities in DMF and magnetic moments of the complexes in the solid state.

Transitions due to *N*-benzoylthiosemicarbazide are characterized by high $\varepsilon_{\max}$ values. The two bands in all metal complexes located at 217–267 and 354–388 nm are assigned to the ($\pi \rightarrow \pi^*$) transitions within the organic ring. The absorption band at 309–324 nm is assigned to ($\pi \rightarrow \pi^*$) transitions for both C=O and C=N groups and at 404–425 nm to the ($n \rightarrow \pi^*$) transition of the oxygen, nitrogen, and sulfur.

The electronic spectrum of the olive green $[Co(L)_2(H_2O)_2] \cdot 2H_2O$ complex (**1**) shows an octahedral geometry; spectra of Co(II) octahedral complexes usually consist of three bands [30]. The first band, due to ${}^4T_{2g}(F) \leftarrow {}^4T_{1g}(F)$, is likely in the near infrared and not observed. The other two bands were in the visible region, due to ${}^4A_{2g}(F) \leftarrow {}^4T_{1g}(F)$ at 615 nm and ${}^4T_{1g}(P) \leftarrow {}^4T_{1g}(F)$ at 490 nm, slightly overlapped with the charge transfer band of the ligand. The Co(II) complex has a magnetic moment of 5.06 B.M. at room temperature, typical for octahedral complexes (4.8–5.2 B.M.) [31]. Molar conductivity of **1** was $9\,\mathrm{Ohm^{-1}cm^2mol^{-1}}$, indicating a non-electrolyte.

The electronic spectrum of the dark green $[Ni(L)_2(H_2O)_2] \cdot 2CH_3OH$ showed a band due to ${}^3T_{1g}(P) \leftarrow {}^3A_{2g}(F)$ at 732 nm and a shoulder at 690 nm. Bands due to ${}^3T_{2g}(F) \leftarrow {}^3A_{2g}(F)$ and ${}^3T_{1g}(F) \leftarrow {}^3A_{2g}(F)$ are expected [30, 32], but not observed because the former overlapped with the ($n \rightarrow \pi^*$) transition and the latter lies in the near infrared. The magnetic moment of 2.92 B.M. lies in the range 2.9–3.3 B.M. for Ni(II) octahedral complexes [31]. The molar conductivity of the Ni(II) complex in DMF was $21\,\mathrm{Ohm^{-1}cm^2mol^{-1}}$, indicating a non-electrolyte. The mass spectrum of **2** showed the molecular ion peak at $m/e$ 483, which agrees with the formula weight (F.W. = 483.28) after subtracting two methanol molecules; the two isotopes of nickel in 2.5 : 1 ratio, two mass unit apart were observed.

The electronic spectrum of the dark blue $[Cu(HL)(NO_3)_2] \cdot CH_3OH$ in DMF showed one unsymmetrical band at 565 nm due to ${}^2A_{1g} \leftarrow {}^2B_{1g}$, ${}^2B_{2g} \leftarrow {}^2B_{1g}$, ${}^2E_g \leftarrow {}^2B_{1g}$ transitions in a square planar geometry [30]. The magnetic moment for **3** was 1.73 B.M., at the lower range of 2.00–1.73 B.M. for square planar structure [33]. The molar conductivity of Cu(II) complex was $83\,\mathrm{Ohm^{-1}cm^2mol^{-1}}$, indicating 1 : 1 ionic complex. DMF is a good donor and can replace the $NO_3^-$ from the coordination sphere of metal complexes [34].

The electronic spectrum of the brown orange $[Fe(L)(NO_3)_2(H_2O)_2] \cdot 2C_2H_5OH$ has weak bands at 740, 605, and 558 nm. It was not possible to identify the type of d–d transitions due to strong charge transfer tailing from UV to the visible region [30, 33], consistent with ligand-metal charge transfer. Elemental analysis and infrared spectrum with coordinated nitrate suggested that compound **5** has octahedral geometry. The magnetic moment value of 5.90 B.M. indicates a high spin octahedral arrangement ($t_{2g}^3 e_g^2$) where the literature magnetic moment is 5.92 B.M. [31]. The molar conductivity value was $91\,\mathrm{Ohm^{-1}cm^2mol^{-1}}$, indicating exchange of coordinated nitrate with DMF [34].

The electronic spectrum of the dark blue $[VO(HL)(SO_4)(H_2O)] \cdot 2CH_3OH$ showed bands at 565 and 500 nm, which correspond to ${}^2E \leftarrow {}^2B_2$ and ${}^2B_1 \leftarrow {}^2B_2$, respectively [33]. In addition, the spectrum shows a band above 410 nm, which may be due to spin charge transfer, consistent with octahedral geometry around VO(IV) ion. Oxovanadium(IV) complex is magnetically simple with a spin only moment of 1.73

B.M.; the actual magnetic moment was 2.1 B.M. The measured molar conductivity of the oxovanadium(IV) complex in DMF solution was 105 $\mathrm{Ohm^{-1}cm^2mol^{-1}}$ due to exchange of DMF with coordinated anion [34].

The electronic absorptions of $[UO_2(L)_2(H_2O)] \cdot 2H_2O$ arise from metal → ligand charge transfer as a broad, intense absorption at 512 nm tailing into the visible region. Compound **8** is diamagnetic as expected [35] and the molar conductivity in DMF was 18 $\mathrm{Ohm^{-1}cm^2mol^{-1}}$, indicating a non-electrolyte.

The white $[Zn(L)_2] \cdot 2H_2O$ (**4**) and $[Cd(L)_2] \cdot 1½\ H_2O$ (**6**) complexes are diamagnetic with molar conductivities in DMF of 16 and 18 $\mathrm{Ohm^{-1}cm^2mol^{-1}}$, respectively, indicating non-electrolytes.

The chemical shifts of the proton signals in the $^1$H-NMR spectrum of the $[Zn(L)_2] \cdot 2H_2O$ (**4**) in DMSO-$d_6$ and their assignments are listed in "Supplementary material". The NH– protons were not observed in the $^1$H-NMR spectrum, indicating deprotonation to coordinate with Zn(II).

### 3.3. *Thermal gravimetric studies*

Thermal gravimetric analysis for $[Ni(L)_2(H_2O)_2] \cdot 2CH_3OH$ and $[Cu(HL)(NO_3)_2] \cdot CH_3OH$ were used as examples to identify the structure of the complexes, especially for coordinated and uncoordinated water and/or methanol molecules [36–38]. Thermal analysis of **2** showed five stages. The first was loss of two uncoordinated methanol molecules (endothermic process, Anal. Calcd/Found%; 6.58/6.56%) at 48.7°C. The second stage was endothermic loss of $C_6H_6$ and $NH_3$ (Anal. Calcd/Found%; 19.47/19.12%) at 191.9°C. The third stage was loss of two water molecules (endothermic, Anal. Calcd/Found%; 9.29/9.78%) at 261.4°C. The fourth and fifth stages were degradation of the rest of the ligands at 360.6 and 480.9°C with weight loss of 23.60 and 20.92%, respectively. Thermal analysis of **3** had three stages; first was loss of one uncoordinated methanol (endothermic process, Anal. Calcd/Found%; 4.255/5.539%) at 53.5°C, the second loss of $N_2O_5$ from degradation of coordinated nitrate (endothermic, Anal. Calcd/Found%; 19.86/18.98%) at 174.4°C and the third was exothermic degradation of the ligand (Anal. Calcd/Found%; 36.75/37.67%).

### 3.4. *ESR studies of copper(II) (3) and oxovanadium(IV) (7) complexes*

X-band ESR spectra of $[Cu(HL)(NO_3)_2] \cdot CH_3OH$ and $[VO(HL)(SO_4)(H_2O)] \cdot 2CH_3OH$ were recorded in the solid state at 25°C. The unresolved hyperfine splitting for Cu(II) can be attributed to dipolar effect caused by mutual interactions between nuclear spin of the (C=N) ($I = 1$) with the unpaired of electron density of Cu(II) [39]. The spin Hamiltonian parameters for [Cu(II)–sq.] ($S = ½, I = \frac{3}{2}$) were calculated. The $g$-tensor values can be used to derive the ground state. In square planar or square pyramidal complexes, the unpaired electron in the $d_{x^2-y^2}$ orbital gives $g_{11} > g_1 > 2.0023$, while $g_1 > g_{11} > 2.0023$, if the unpaired electrons lies in $d_{z^2}$ orbital; the observed values of $g_{11}$ (2.2451) $> g_1$ (2.1221) $> 2.0023$ indicate a $d_{x^2-y^2}$ ground state characteristic for square planar [40].

The $g_{11}$ value is an important function for indicating the covalent character of (M–L) bonds [41]. For ionic, the $g_{11}$ is $< 2.0023$ while for covalent $g_{11}$ is $> 2.0023$. In the

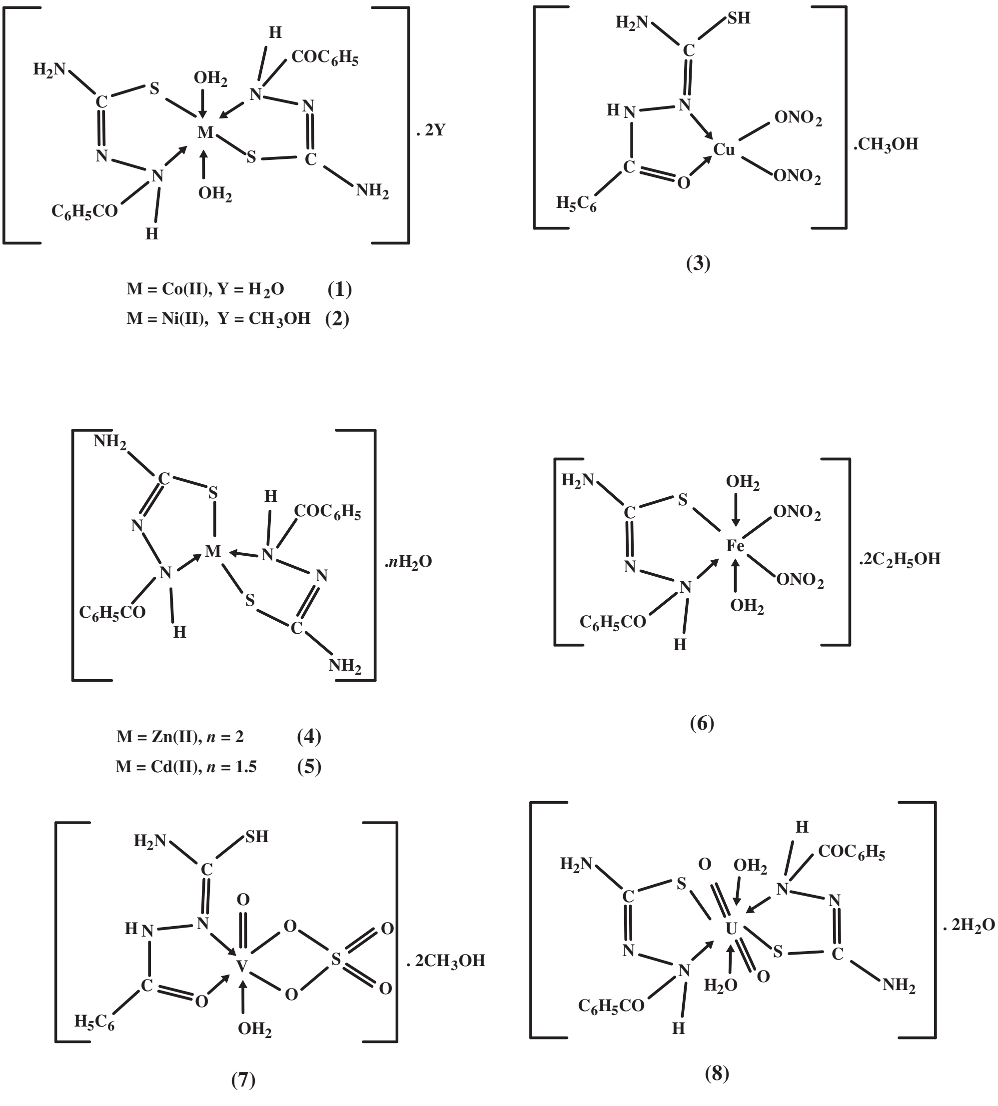

M = Co(II), Y = $H_2O$ (1)
M = Ni(II), Y = $CH_3OH$ (2)

(3)

M = Zn(II), n = 2 (4)
M = Cd(II), n = 1.5 (5)

(6)

(7)

(8)

Figure 3. Structures of the metal complexes with *N*-benzoylthiosemicarbazide.

present complex, $g_{11}$ is more than 2.0023, indicating covalent Cu–L bond. In axial symmetry, the $g$-values are related to the $G$-factor by the expression $G = (g_{11} - 2)/(g_1 - 2)$. According to Hathaway [42], if $G > 4$, the exchange interaction between Cu(II) centers in the solid state is negligible, but when $G < 4$, considerable exchange is indicated. The $G$ value of **3** suggests the absence of exchange coupling between Cu(II) centers in the solid state [43]. The powder ESR spectrum of Cu(II) complexes is typical for square planar [44]. The value of the magnetic moment ($\mu = 1.73$ B.M.) and spectral data (565 nm) agree with square planar structure.

The X-band ESR spectrum of powdered sample of **7** at room temperature gave a broad line centered on $g = 2.1103$ and without resolved $^{51}V$ ($I = \frac{7}{2}$, $S = \frac{1}{2}$) hyperfine structure. The absence of vanadium's hyperfine coupling is common in the solid state

Table 4. Biological activity of the synthesized *N*-benzoylthiosemicarbazide, HL, ligand, and **1**–**8**.

| | Mean of zone diameter[a] (mm) | | | | | | | | | | | |
|---|---|---|---|---|---|---|---|---|---|---|---|---|
| | Gram-positive bacteria[b] | | | | Gram-negative bacteria[b] | | | | Fungi[c] | | | |
| Organisms | *S. aureus* (ATCC 25923) | | *S. pyogene* (ATCC 19615) | | *P. phaseolicola* (GSPB 2828) | | *P. fluorescens* (S 97) | | *F. oxysporum* | | *A. fumigatus* | |
| | **A** | **B** | **A** | **B** | **A** | **B** | **A** | **B** | **A** | **B** | **A** | **B** |
| HL · $^1/_2$HCl | 12 | 5 | 9 | 8 | 10 | 6 | 7 | 2 | 4 | 3 | 6 | 5 |
| **1** | 11 | 7 | 11 | 5 | 5 | 2 | 12 | 7 | 7 | 7 | 11 | 9 |
| **2** | 13 | 3 | 7 | 3 | 4 | 5 | 10 | 6 | 10 | 6 | 9 | 6 |
| **3** | 8 | 6 | 6 | 4 | 7 | 8 | 8 | 3 | 5 | 8 | 8 | 7 |
| **4** | 7 | 5 | 10 | 7 | 10 | 7 | 5 | 7 | 8 | 5 | 5 | 3 |
| **5** | 12 | 5 | 12 | 9 | 4 | 3 | 7 | 4 | 11 | 8 | 9 | 7 |
| **6** | 13 | 7 | 8 | 6 | 7 | 8 | 4 | 4 | 6 | 6 | 6 | 4 |
| **7** | 10 | 6 | 12 | 6 | 22 | 16 | 20 | 14 | 9 | 3 | 9 | 8 |
| **8** | 28 | 20 | 31 | 23 | 30 | 23 | 30 | 24 | 3 | 7 | 11 | 9 |
| Control # | 42 | 28 | 38 | 30 | 36 | 25 | 38 | 30 | 40 | 28 | 40 | 31 |

[a] Chloramphencol in the case of Gram-positive bacteria, cephalothin in the case of Gram-negative bacteria, and cycloheximide in case of fungi. The concentration A is $2\,\mathrm{mg\,mL^{-1}}$ and B is $1\,\mathrm{mg\,mL^{-1}}$.

[b] Calculated from 3 values.

[c] Identified depending on morphological and microscopical characteristics.

[22] and is attributed to the simultaneous flipping of neighboring electron spin [45] or strong exchange interactions, which average out the interaction with the nuclei. For octahedral complex the shape of the spectrum, spectral studies, and magnetic moment ($\mu = 2.1$ B.M.) agree with proposed structures.

From elemental analysis, infrared, mass, electronic, and ESR spectra, and TGA analysis, tentative structures of the metal complexes are provided in figure 3.

### 3.5. *Antimicrobial activity*

Using the agar cup method in DMF at $2\,\mathrm{mg\,mL^{-1}}$ and $1\,\mathrm{mg\,mL^{-1}}$, ligand and complexes were checked against *S. aureus*, *S. pyogenes*, *P. fluorescens*, and *P. phaseolicola*. Zone of inhibition diameters (in mm) of standard antibiotics chloramphencol, cephalothin, and cycloheximide were used as standards for Gram-positive, Gram-negative bacteria, and antifungal. Most metal complexes have low activity towards Gram-positive bacteria and fungi (table 4). Complex **8** showed high antibacterial activity against both Gram-positive and Gram-negative bacteria, while **7** has moderate antibacterial activity. These compounds showed no effect against fungi.

## 4. Conclusion

*N*-Benzoylthiosemicarbazide was synthesized by fusion of benzoylhydrazide and ammonium thiocyanate. The ligand is either neutral or monobasic bidentate coordinating through NS or NO sites. The ligand and its metal complexes were screened towards antimicrobial activity.

## References

[1] J.S. Casasm, M.S. Garsia-Tasende, J. Sordo. *Coord. Chem. Rev.*, **209**, 197 (2000).
[2] V.M. Leovac, V.I. Češljević. *Coordination Chemistry of Isothiosemicarbazides and Their Derivatives*, University of Novi Sad, Novi Sad, New Delhi (2002).
[3] B. Neelam, M. Mannar, R.N. Fehmida, B. Alok, B. Sudha, A. Amir. *Europ. J. Med. Chem.*, **35**, 481 (2000).
[4] M.B. Ferrari, F. Bisceglie, G. Pelosi, M. Sassi, P. Tarasconi, M. Cornia, S. Capacchi, R. Albertini, S. Pinelli. *J. Inorg. Biochem.*, **90**, 113 (2002).
[5] D.X. West, A.E. Liberta, S.B. Padhye, R.C. Chikate, P.B. Sonawane, A.S. Kumbhar, R.G. Yeranade. *Coord. Chem. Rev.*, **123**, 49 (1993).
[6] D. Kovala-Demertzi, P.N. Yadav, M.A. Demertzis, J.P. Jasiski, F.J. Andreadaki, I.D. Kostas. *Tetrahedron Lett.*, **45**, 2923 (2004).
[7] D. Kovala-Demertzi, M.A. Demertzis, E. Filiou, A.A. Pantazaki, P.N. Yadav, J.R. Miller, Y. Zheng, D.A. Kyriakidis. *Biometals*, **16**, 411 (2003).
[8] D. Kovala-Demertzi, A. Boccarelli, M.A. Demertzis, M. Coluccia. *Pharmacology*, **53**, 148 (2007).
[9] R.B. Singh, B.S. Garg, R.P. Singh. *Talanta*, **25**, 619 (1978).
[10] R.B. Singh, I. Ishii. *Cryst. Rev. Anal. Chem.*, **22**, 381 (1991).
[11] A.A. El-Asmy. *Bull. Soc. Chim. Fr.*, **2**, 171 (1989).
[12] M.M. Mostafa, A.M. Shallaby, A.A. El-Asmy. *Transition Met. Chem.*, **6**, 303 (1981).
[13] A.A. El-Asmy, T.Y. Al-Ansi, R.R. Amin, M. Mourin. *Polyhedron*, **9**, 2029 (1990).
[14] M. Abram, E.S. Lang, E. Bonfada. *Z. Anorg. Allg. Chem.*, **628**, 1419 (2002).
[15] H.D. Bian, G.Q. Guo, Q. Yu, H. Liang, X.E. Yang, L.G. Zhu. *Acta Cryst.*, **E61**, 639 (2005).
[16] H.A. Flaschka. *EDTA Titration*, 2nd Edn, p. 81, Pergamon Press, New York (1964).
[17] A.I. Vogel. *Textbook of Quantitative Inorganic Analysis*, 4th Edn, Longman, London (1978).
[18] T.S. West. *Complexometry with EDTA and Related Reagents*, 3rd Edn, DBH Ltd., Pools (1969).
[19] F.E. Mabbs, D.J. Machin. *Magnetism and Transition Metal Complexes*, Dover Publications, New York (2008).
[20] D.C. Gross, S.E. De Vay. *Physiol. Plant Pathol.*, **11**, 13 (1977).
[21] A.W. Bauer, W.W.M. Kirby, J.C. Sherris, M. Turck. *Am. J. Clin. Pathol.*, **45**, 493 (1966).
[22] A.A. Abou-Hussen, N.M. El-Metawally, E.M. Saad, A.A. El-Asmy. *J. Coord. Chem.*, **58**, 1735 (2005).
[23] F.A. El-Said, A.A. El-Asmy, W. Kaminsky, D.X. West. *Transition Met. Chem.*, **28**, 954 (2003).
[24] R.J. Platt. *J. Chem. Phys.*, **17**, 484 (1949).
[25] E. Pretsch, J. Seibl. *Tables of Spectral Data for Structure Determination of Organic Compounds*, Springer-Verlag, Berlin (1983).
[26] A.A.A. Abou-Hussen, A.A.A. Emara. *J. Coord. Chem.*, **57**, 973 (2004).
[27] A.A.A. Emara, O.M.I. Adly. *Transition Met. Chem.*, **32**, 889 (2007).
[28] A.A.A. Emara, A.A. Saleh, O.M.I. Adly. *Spectrochim. Acta, Part A*, **68**, 592 (2007).
[29] K. Nakamoto. *Infrared Spectra of Inorganic and Coordination Compounds*, 5th Edn, John Wiley & Sons, New York (1997).
[30] N.N. Greenwood, A. Earnshaw. *Chemistry of the Elements*, Pergamon Press, New York (1984).
[31] F.A. Cotton, G. Wilkenson. *Advanced Inorganic Chemistry. A Comprehensive Text*, 4th Edn, John Wiley and Sons, New York (1986).
[32] A.E. Martell. *Coordination Chemistry*, Vol. 1, Van Nostrand Reinhold Co., New York (1971).
[33] J.C. Bailar, H.J. Emeleus, R. Nyholm, A.F. Trotman-Dickenson. *Comprehensive Inorganic Chemistry*, Vol. 3, Pergamon Press, New York (1975).
[34] W.J. Geary. *Chem. Rev.*, **7**, 8 (1971).
[35] E. Rabinowitch, R.L. Belford. *Spectroscopy and Photochemistry of Uranyl Compounds*, Pergamon Press, New York (1984).
[36] A.A.A. Emara, F.S.M. Abd El-Hameed, S.M.E. Khalil. *Phosphorus, Sulfur, and Silicon*, **114**, 1 (1996).
[37] S. Rehman, M. Arshad, S.A. Khan, K. Masud, N. Arshad, A.H. Qureshi, S.A. Ghauri. *Thermochim. Acta*, **345**, 81 (2000).
[38] S. Khan, C.J. Anwar, M. Arshad, K. Masud. *Radiochim. Acta*, **94**, 853 (2006).
[39] G.A.A. Al-hazmi, M.S. El-Shahawi, I.M. Gabr, A.A. El-Asmy. *J. Coord. Chem.*, **58**, 713 (2005).
[40] G. Speie, J. Csihony, A.M. Whalen, C.G. Repant. *Inorg. Chem.*, **35**, 3519 (1996).
[41] J.P. Jasinski, J.R. Bianchani, D.X. West. *Z. Anorg. Allg. Chem.*, **629**, 202 (2003).
[42] B.J. Hathaway. *Structure and Bonding (Berlin)*, **57**, 551 (1984).
[43] B.J. Hathaway, D.E. Billing. *Coord. Chem. Rev.*, **5**, 143 (1970).
[44] M.L. Miller, S.A. Ibrahim, M.L. Golden, M.Y. Darensbourg. *Inorg. Chem.*, **42**, 2999 (2003).
[45] A. Bencini, D. Gattechi. *EPR of Exchange Coupled Systems*, Springer Verlach, Berlin (1990).